Ensemble simulation of the lightning flash variability in a 3D cloud model with parameterizations of cloud electrification and lightning flashes

Jean-Pierre Pinty, Christelle Barthe

NOTES AND CORRESPONDENCE

Ensemble Simulation of the Lightning Flash Variability in a 3D Cloud Model with Parameterizations of Cloud Electrification and Lightning Flashes

JEAN-PIERRE PINTY AND CHRISTELLE BARTHE*

Laboratoire d'Aérologie, University of Toulouse, CNRS UMR 5560, Toulouse, France

(Manuscript received 1 March 2007, in final form 4 May 2007)

ABSTRACT

A series of ensemble simulations were performed to study the statistics of flash characteristics produced by an electrification and lightning scheme in the cloud-resolving model Méso-NH. Here, the electrical variability of two storms—one supercellular and one multicellular—results from a random triggering location of the flashes and from a branching algorithm that describes the flash path. The study shows that the electrical model is able to generate several estimates of the total flash number for an identical evolution of the dynamics and microphysics of each storm in the 120 ensemble members. The variability of the flash number spans over three standard deviations taken from the ensemble mean. The simulations produce regularly shaped distributions of flash internal parameters (i.e., number of segments and branching levels per flash). The ensemble simulation shows that the model is stable and self-regulatory as suggested by the limited overshoot on the maximum electric field time series. An application to the production of nitrogen oxides indicates that the two storms produce 200 ± 150 mol of NO per flash on average.

1. Introduction

The simulation of lightning flash parameters (location, frequency, length, polarity, peak current, etc.) is undoubtedly a difficult task; even the origin of cloud electrification (the inductive and noninductive charge separation processes) is still not fully understood. Consequently, the driving charging mechanisms are highly parameterized, which leads to known uncertainties in cloud electrification models as concluded by Helsdon et al. (2001), Mansell et al. (2005), Altaratz et al. (2005), and Barthe and Pinty (2007b). Concerning the lightning flashes more precisely, it is even questionable whether flash characteristics could be correctly resolved with a pure deterministic algorithm. For instance, Mansell et al. (2002) showed that the seminal model of dielectric breakdown of Niemeyer et al. (1984) is well suited to simulating electrical discharges in the atmosphere, with lightning channels segmented in a fractal structure with branches. Dielectric breakdown models are based on the step-by-step probabilistic growth of a structure that propagates preferentially in cloudy regions of high charge density. The extension of the structure from a grid point on the channel is chosen randomly and according to the local value of the electric field. This picture of flash growth was also adopted by Barthe et al. (2005) and Barthe and Pinty (2007a), but after simplification for computational efficiency. In this model, the lightning scheme is directly based on a fractal geometry analog to generate the skeletal structure of the flashes. In summary, a common ingredient of these recent lightning schemes is the probabilistic nature of their branching algorithm. This feature leads to an inherent variability of the flash characteristics, which have not been evaluated so far.

Beyond the propagation of the flashes, another uncertainty, which stems from discharge models, is the undetermined location of the flash initiation. In the model of Barthe and Pinty (2007a), lightning is initiated

* Current affiliation: National Center for Atmospheric Research, Boulder, Colorado.

Corresponding author address: Jean-Pierre Pinty, Laboratoire d'Aérologie, CNRS, Université Paul Sabatier Toulouse III, UM5560, 14 av. Edouard Belin, 31400 Toulouse, France.
E-mail: pinjp@aero.obs-mip.fr

DOI: 10.1175/2007MWR2186.1

when the magnitude of the electric field at any grid point of the cloud reaches a threshold value corresponding to the breakeven electric field estimated by Marshall et al. (1995) from electric field soundings. Moreover, and as discussed by MacGorman et al. (2001), an additional 10% reduction of the threshold can be considered to approximate a subgrid-scale variability of the computed electric field. As a result, the location of the flash triggering point is chosen at random among the grid points that fall in the 10% range below the breakeven threshold.

A simple way to generate statistics of lightning flash variability is to investigate an ensemble simulation technique pioneered by Houtekamer and Derome (1995) for a Monte Carlo–like simulation of the impact of random observational errors in a data assimilation system. In the present study the ensemble members are obtained in a very straightforward manner because they only reflect the natural variability of the flash triggering and branching algorithms. Therefore, in all the storm simulations, the dynamics and the microphysics are not perturbed because no feedback of the electrification scheme is considered for the moment. Strictly imposing the same dynamical and microphysical evolution on the ensemble members also implies the same electrical forcing through the noninductive charging process. This is not the case however for the inductive process that depends on the local amplitude and orientation of the electric field, which may vary among the ensemble members.

In this study, we analyze the results of two electrified storms: one supercellular and one multicellular (Barthe and Pinty 2007a,b), for which 120 simulations have been performed with the mesoscale model Méso-NH, here run at moderately high resolution. In section 2, we briefly describe these two cases. The ensemble simulation results are analyzed in sections 3 and 4. Some conclusions are drawn about the related consequences on the uncertainties of the flash characteristics.

2. Case studies

Two different idealized storm cases were examined: a supercellular storm and a multicellular storm. Details about these two storms can be found in Barthe et al. (2005) and Barthe and Pinty (2007a,b), but the initialization of both storms is recalled in this section.

The model domain of the multicellular storm has $40 \times 40 \times 36$ grid points with a horizontal spacing of 1 km, and a constant vertical resolution of 500 m. The time step is 2 s and the duration of the simulation is 100 min. Convection is initiated by placing a warm bubble (+2 K) of radius 10 km at 10 and 22.5 km from the west and north boundaries of the domain of simulation, respectively. The vertical profiles of temperature and moisture are taken from Weisman and Klemp (1984). The initial wind profile of the first 5 km above the ground is taken from a half-circle hodograph with an arc radius, equal to 20 m s^{-1}. The wind keeps its easterly direction and its magnitude above 5 km. This multicellular storm will be referred to as WK84 in what follows.

The simulation of the supercellular storm lasted 80 min, and the domain was 40 km $\times$ 40 km $\times$ 30 grid points with a resolution of 1 km on the horizontal scale and 500 m on the vertical. Convection was initiated by a warm bubble located in the planetary boundary layer, in the southwestern corner of the domain. The initial sounding came from Klemp and Wilhelmson (1978). The idealized hodograph was characterized by a vertical shear with a low-level veering wind and an upper-level wind constant in speed and direction (southwestern flow). This supercellular storm will be referred to as KW78 hereafter.

For both storms, 120 simulations were performed with the same model and the same initial conditions. The variability in the results comes from the stochastic character of the lightning flash scheme, which only altered the electrical state of each simulated storm.

These two storms had very different electrical characteristics. The cloud top of the supercellular storm reached only 8–9 km, and the maximum vertical velocity did not exceed 18 m s^{-1}. This storm exhibited an inverted electrical structure with a negative layer of charge above a positive layer. The multicell electrical structure was a tripole (positive, negative, positive stacked structure), and the cloud top and the maximum vertical velocity were 14 km high and 56 m s^{-1} respectively. Therefore, it is interesting to examine the flash statistics of these contrasted storm simulations.

3. Model configuration

The model has explicit microphysics with prediction of the mixing ratio of two liquid and three ice categories of condensate (Barthe et al. 2005). The electric charges are carried by each type of hydrometeor. Inductive and noninductive mechanisms are both considered. The Takahashi (1978) noninductive charge separation parameterization is used in all the simulations. The electrical scheme produces both intracloud (IC) and cloud-to-ground (CG) flashes with details given in Barthe and Pinty (2007a).

We reiterate here that the dynamics and the microphysical aspects of the simulations are identical in each storm case. The variability of the ensemble simulation

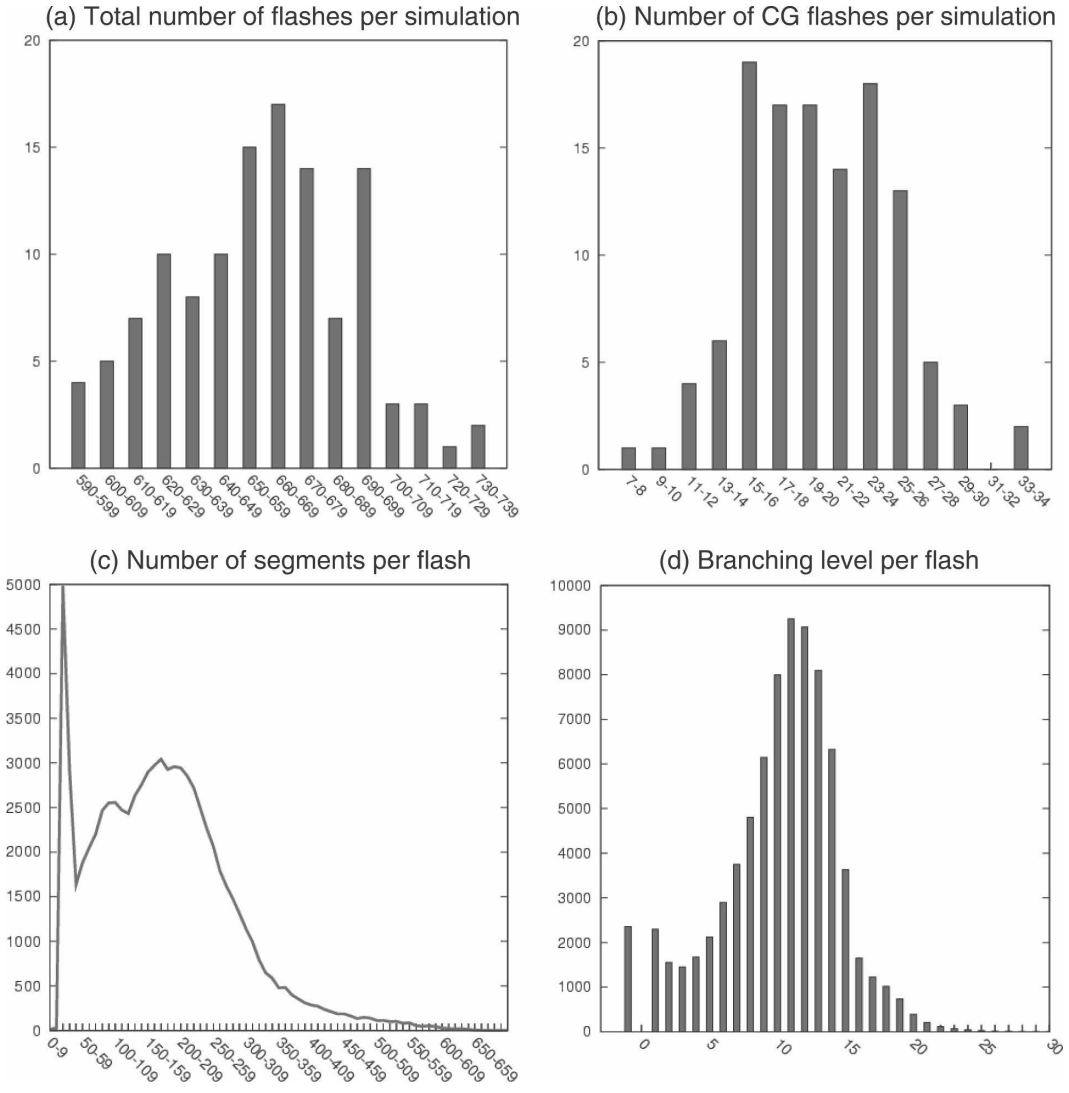

FIG. 1. (a) Histogram of the total number of lightning flashes per simulation and (b) of the number of CG flashes per simulation, (c) distribution of the number of segments per flash, and (d) histogram of the branching level per flash for the WK84 ensemble experiment. Statistics were obtained using 120 simulations for (a) and (b), and with 78 929 lightning flashes for (c) and (d). The horizontal axis corresponds to the classes defined for each histogram. The vertical axis shows the number of events for a given class. The −1 branching level in (d) highlights the unbranched flash case.

is the result of the probabilistic treatment of the flash triggering and propagation.

4. Simulated lightning flash statistics

a. Multicellular storm

Figure 1a shows the histogram of the number of flashes per simulation. The total number of flash ranged between 590 and 740 with a mean value of 658 flashes per simulation. The uncertainty was 23% and the standard deviation was 32 flashes. Nearly 90% of the simulations produced a total number of flashes between 600 and 699. A larger variability was observed for the number of CG flashes (Fig. 1b). The number of CG flashes per simulation was in the range of 6–35 with a mean value of 20. Note that 90% of the simulations had a quasi-uniformly distributed number of CG flashes between 14 and 29 (Fig. 1b). However, although the variability of the CG number per simulation was high, their proportion, between 1% and 5% of the total flash number, was low.

A large variability was found for the number of segments forming the individual lightning flashes (Fig. 1c).

TABLE 1. Summary of the mean value (M) and standard deviation (σ) for each set of simulations. WK84 refers to the multicellular storm from Weisman and Klemp (1984) and KW78 refers to the supercellular storm from Klemp and Wilhelmson (1978).

	WK84		KW78	
	M	σ	M	σ
Tot No. of flashes per simulation	658	32	358	16
No. of CG flashes per simulation	20	5	32	5
CG/IC ratio ($\times 10^{-2}$)	3.2	0.8	9.7	1.6
Branching level per flash	10.1	4.4	7.4	2.3
No. of segments per flash	177	107	113	55
Triggering electric field for CG (kV m^{-1})	108.8	11.5	121.2	7.0
Triggering electric field for IC (kV m^{-1})	95.3	16.0	117.4	8.5
Triggering altitude for CG (m)	5745	801	4715	336
Triggering altitude for IC (m)	7173	1344	5033	441

The number of segments per flash varied between 3 and 650 with a mean value of 113 (the total flash length was estimated as the number of segments times the cube root of the model gridcell volume). The simulated flash length distribution was consistent with observations taken from the Office National d'Etudes et de Recherches Aérospatiales (ONERA) interferometer operating during the 10 July Stratosphere–Troposphere Experiment: Radiation, Aerosols, and Ozone (STERAO) storm. For instance, Defer et al. (2003) showed that the total flash length of individual flashes lays between 0.02 and 494 km with a mean value of 19 km. Figure 1c also shows that a large proportion of flashes had between 10 and 29 segments (close to 8–25 km in length). These "shorter" flashes are consecutive to highly branched intracloud flashes with many segments that instantaneously neutralize a large amount of charge. Defer et al. (2003) have observed "short duration flashes" during the STERAO field campaign, but there is still debate about the realism and the physics of these observed discharges.

A histogram of flash branching level is presented in Fig. 1d. The branching level is an indicator of the flash horizontal extension. By definition, a branching level of rank 0 corresponds to the bidirectional leader. A branching level of rank 1 labels the branches directly linked to the bidirectional leader, then branches of rank 2 are those linked to branches of rank 1, and so on. We refer to Barthe et al. (2005) and Barthe and Pinty (2007a) for the details of the branching algorithm. Figure 1d shows that the branching level per flash peaked between 11 and 12, which means that flashes were densely branched, even at the moderate resolution of the model. It can be seen that the ensemble of 120 simulations produced 2300 unbranched flashes with a single bidirectional leader (here plotted with -1 branching level to show them up). These flashes were followed by 2200 poorly branched flashes of rank 1, which propagated over a short distance in residual electric charge pockets.

Additional results of the ensemble simulation are summarized in Table 1. The lightning triggering height analysis showed that the CG flashes were initiated at lower altitude (5745 $\pm$ 801 m) than the IC flashes (7173 $\pm$ 1344 m). This partially explains why more IC flashes are triggered, because the exponential decrease of the breakeven electric field with altitude (Marshall et al. 1995) leads to a lower threshold for the IC flashes (95.3 $\pm$ 16.0 kV m^{-1}) compared with that of the CG flashes (108.8 $\pm$ 11.5 kV m^{-1}).

b. *Supercellular storm*

Results obtained for the supercellular storm were comparable to those of the multicellular storm. For the KW78 simulations, the total flash number per simulation was in the range of 320–390 with a mean value of 358 $\pm$ 16 (see Table 1). The proportion of CG flashes was higher (32 $\pm$ 5). Also, as noted by Barthe and Pinty (2007b), the multicellular storm presents a tripolar structure, while the supercellular storm is an inverted dipole. Therefore, the flashes in the multicell storm are triggered either between the upper positive charge and the central negative charge or between the negative charge and the positive charge at lower level. This explains why the standard deviation of the IC flash triggering altitude was 3 times that found for the supercell storm (1344 m against 441 m in Table 1). Another difference between the two storms concerns the distribution of the number of segments per flash (cf. Figs. 1c and 2c). The supercellular storm did not produce the short flash category that showed up in the multicellular case. This difference can be interpreted by considering two arguments. First, the cloud structure of these two storms is very different. The multicellular storm is more horizontally and vertically extended, thus the interface between two regions of opposite charge is larger. The higher charge densities are concentrated around the convective core. So, even if the electric field is locally higher than the propagation threshold, the relatively low charge density in this region cannot sustain the propagation of a highly branched flash. Second, as the supercellular storm is less vigorous, the cloud top was lower so a higher electric field was needed to trigger a

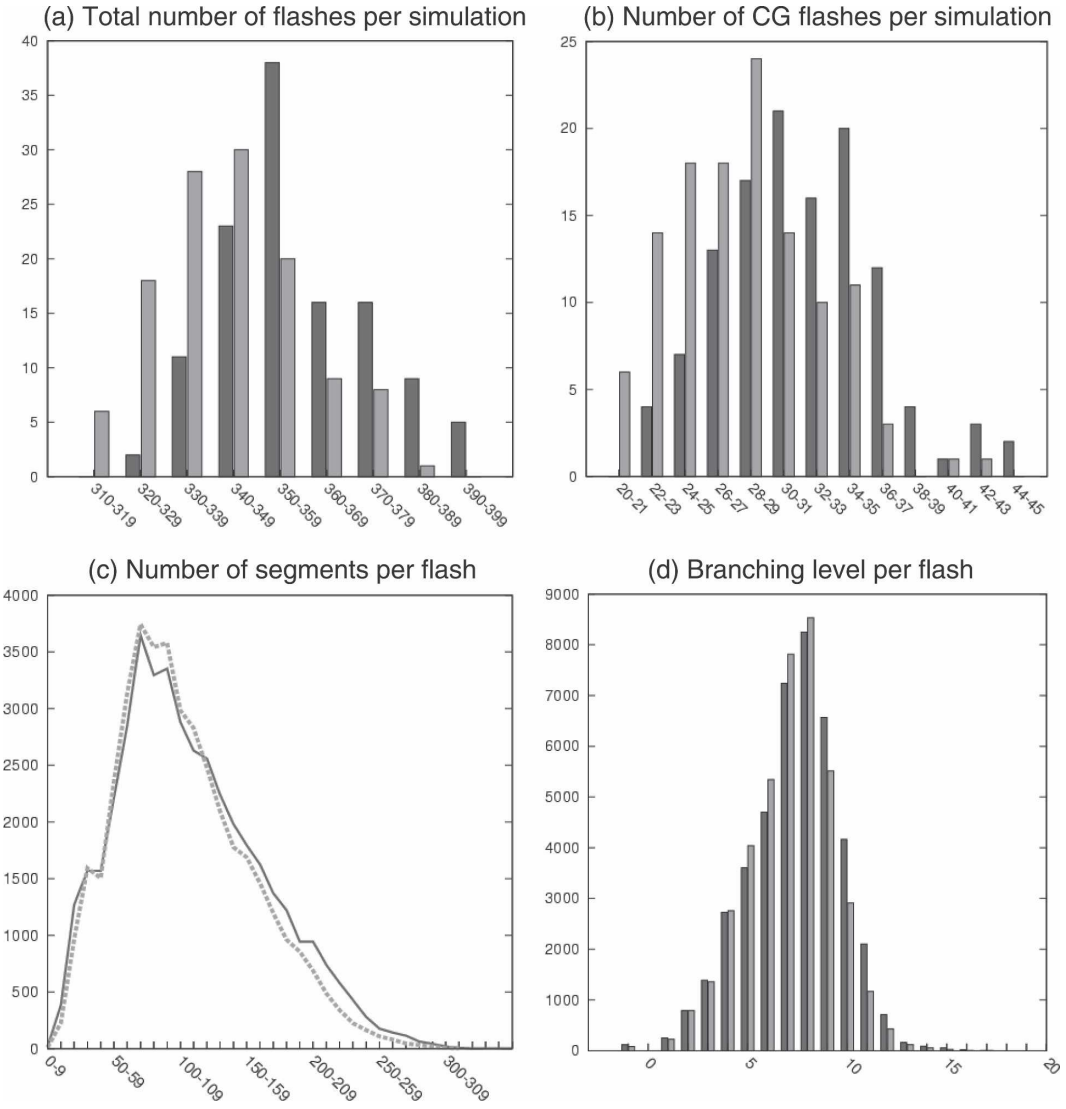

FIG. 2. Same as in Fig. 1, but for the KW78 (black bars and solid line) and for the KW78 without inductive charging processes (gray bars and dotted line) ensemble experiments. (c), (d) Statistics were done with 42 962 (KW78 case) and 41 187 (KW78woI case) flashes for the plots.

flash. It means that the charge density is quite high, and the lightning flash can propagate far from the initiation point.

c. *Impact of the inductive process*

The impact of the inductive process was also examined using two series of 120 simulations of the same supercellular storm. The series differed by including or excluding the inductive charging process. Very few differences were related to the intrinsic flash characteristics (number of segments and branching level distributions). However, the simulations taking into account the inductive charging mechanism tended to produce more flashes (total number and CG; Mansell et al. 2005). This can be related to the simulated shift of the triggering altitude toward the lower altitudes.

5. Electric field limitation

The temporal evolution of the electric field peak value is shown in Fig. 3 for the series of 120 simulations. The electric field is a good indicator of the lightning flash scheme efficiency because neutralizing the charges reduces the total charge density and so limits the growth of the electric field. Figure 3 shows that the lightning scheme was efficient all throughout the dura-

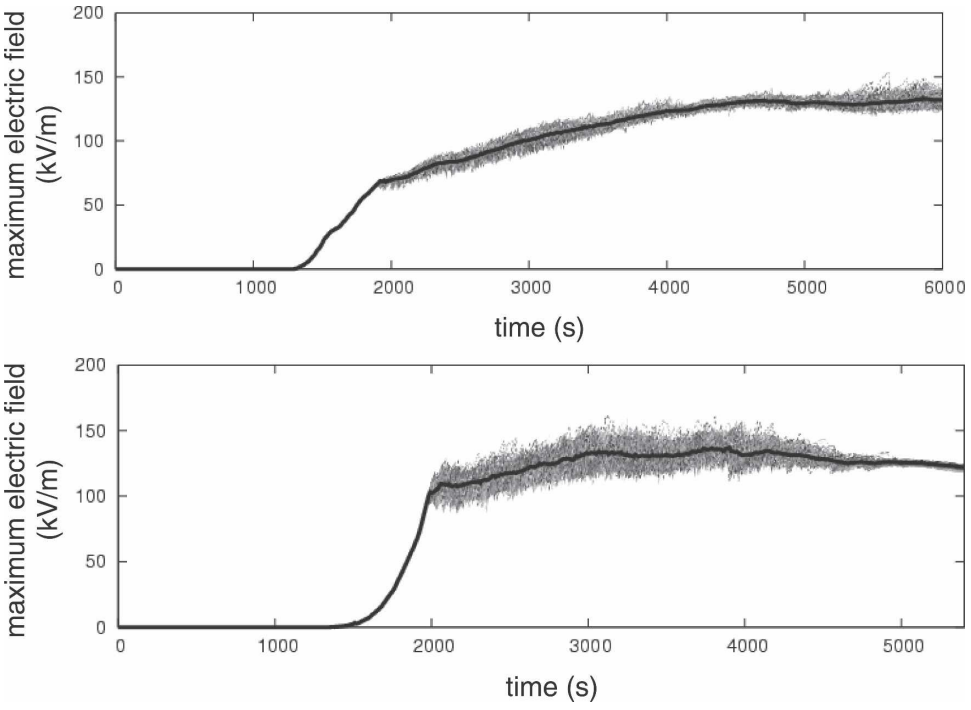

FIG. 3. Temporal evolution of the maximum electric field for the (top) WK84 and (bottom) KW78 experiments. The black line represents the maximum electric field averaged over the 120 simulations.

tion of the storm. A variation of the maximum electric field, up to 40%, was observed during the mature stage of the KW78 simulations. The lightning flash activity ceased after 5100 s in any case. This produced a remarkable convergence of the maximum electric field magnitude at the end of the KW78 simulations. Less variability (~25%) was observed for the WK84 simulations for which a residual electrical activity persisted.

The electric field variability was higher in the KW78 case compared with the WK84 case, as explained by the different vertical extent of these two storms. The KW78 storm was a supercell storm with a maximum vertical velocity of 18 $m\,s^{-1}$ and a cloud-top height reaching 9 km in the mature stage. The multicellular storm WK84 was stronger, with a cloud-top height around 14-km altitude and a maximum updraft velocity exceeding 50 $m\,s^{-1}$. Consequently, the parameterized noninductive charge separation process was more active at the elevated −20°C isotherm level (WK84 storm case) than the −10°C isotherm level of the KW78 storm case. As a charge region at lower altitude implies a higher breakeven electric field and also because fewer flashes are triggered, the KW78 ensemble simulation presented a higher variability of the electric field.

6. Impact on lightning-produced NO_x flux

Lightning flashes provide a major contribution to the nitrogen oxide (NO_x) budget. This has been recognized despite the large uncertainty attached to this source, hereafter referred to as the LNO_x source (Lee et al. 1997). Lightning flashes are efficient because LNO_x is emitted in the mid–upper troposphere where its lifetime is longer and where it is directly available for ozone production. Here, the aim is to evaluate the LNO_x production rate uncertainty due to the probabilistic treatment of the lightning flashes in Méso-NH.

Figure 4 shows the temporal evolution of the NO_x (LNO_x) flux through the anvil for the two series of 120 simulations [see Barthe et al. (2007) for the computation of the flux]. In the WK84 case, the LNO_x fluxes progressively diverged from the ensemble mean value after 3000 s of simulation, so 15 min after initiation of the first flash. At the end of the simulations, the LNO_x flux through the anvil was $4 \times 10^{-7} \pm 0.5 \times 10^{-7}$ mol $m^{-2}\ s^{-1}$, which means an overall variability of 25%. Concerning the KW78 set of simulations, the same flux peaked at $1 \times 10^{-6} \pm 0.5 \times 0^{-7}$ mol $m^{-2}\,s^{-1}$ at the end of the simulation. Here, the lower LNO_x variability (10%) was probably linked to the lower variability of the flash number and flash length in the KW78 simulations.

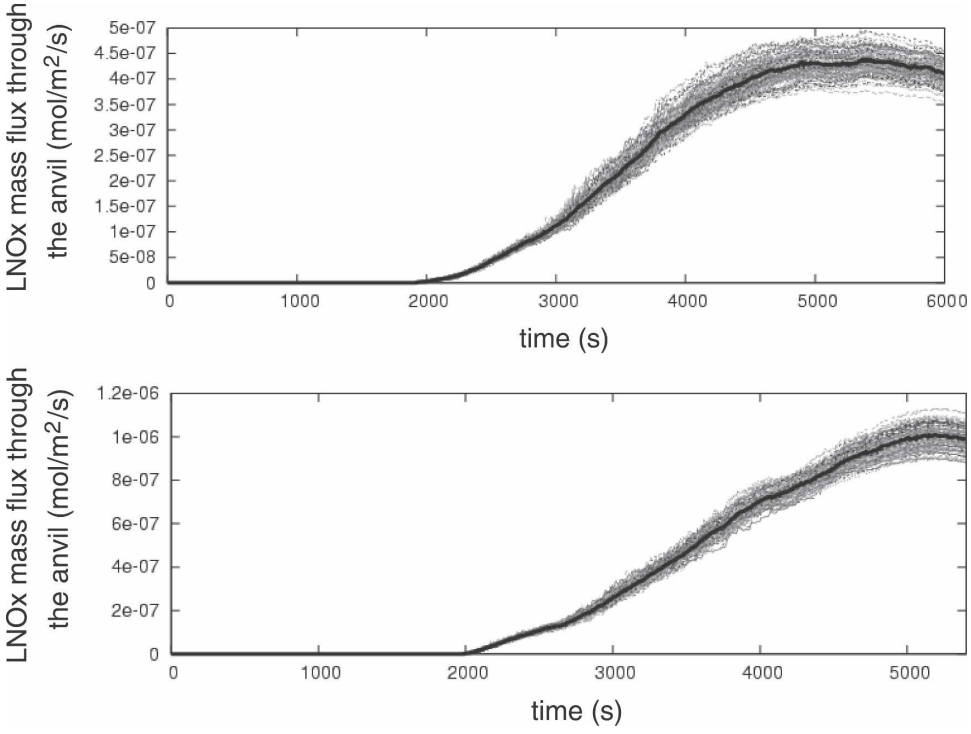

FIG. 4. Temporal evolution of the lightning-produced NO_x mass flux through the anvil for the (top) WK84 and (bottom) KW78 experiments. The black curve represents the LNO_x mass flux averaged over the 120 simulations.

The model calculates the number of NO moles produced per flash using the equation of Wang et al. (1998), which depends on the length of the flash segment and on the local air pressure. In the following bulk analysis, we consider the air pressure at the mean flash triggering altitude (~400 hPa for WK84 and ~500 hPa for KW78). For the WK84 ensemble case, a total flash length of 14×10^9 m and a total flash number of 78 929 for the 120 simulations yield an estimate of 250 ± 142 mol of NO per flash. The range of NO moles per flash is large, between 20 and 850 mol. The upper bound corresponds to a very long flash with more than 600 segments and that has a marginal occurrence according to Fig. 1c. In the case of the KW78 simulations, a total flash length of 4.84×10^9 m and a total flash number of 42 962 were obtained so the estimated LNO_x production is 185 ± 90 mol of NO per flash. The range is between 3 and 490 mol of NO. A value of 3 mol of NO per flash is associated with very short flashes (less than 2 km), which are clearly not very efficient at producing NO. Therefore a gross estimate of the LNO_x efficiency per flash is around 200 ± 150 mol of NO, based on the lightning flash length approach of Wang et al. (1998). This value is consistent with observations from different field campaigns and simulated severe storms (Huntrieser et al. 1998; Skamarock et al. 2003; Fehr et al. 2004; DeCaria et al. 2005; Barthe et al. 2007; Ott et al. 2007).

7. Conclusions

An ensemble simulation of two storms has been performed with a three-dimensional model of cloud electrification. The variability of the simulated electrical properties comes from the lightning scheme where probabilistic aspects are introduced, first to catch the poorly determined location where flashes are triggered, and second to describe the branched structure of the flashes.

The results show that a significant variability of the electrical activity of the two storms (a tripole and an inverted dipole) can be generated while keeping the same dynamical and microphysical framework. Running with the same cloud environment is important to separate an equal amount of electric charge in this ensemble simulation study. The resulting distribution of the total flash number is bounded and spreads over three standard deviations approximately. The standard deviation of the total flash number roughly represents 5% of the ensemble mean value (several hundreds of flashes). A variable number of flash is at the origin of a variability of the electric field. However, the spread of

this variability is internally regulated by the electrical scheme itself because no unrealistic growth of charge density, electric field, or flash rate was noted in any simulation. Finally, the ensemble simulation was applied to estimate the uncertainty of the LNO_x production rate. The two storms typically produced 250 ± 142 and 185 ± 90 mol of NO per flash.

The ensemble simulation shows an interesting potential to point out the consequences of some unavoidable random aspects of the physics of the lightning. The next step is to include little flash variability in cloud-resolving models and in the parameterization of cloud electrical properties for mesoscale and global models to obtain a better estimate of the total flash count and LNO_x emission. Finally, it would be interesting to confirm and to extend these simulation results by comparing them with statistics produced by observed flashes with a high-resolution lightning mapping detector (Krehbiel et al. 2000).

Acknowledgments. The technical support for this research was provided by Didier Gazen and Juan Escobar (both at Laboratoire d'Aérologie) who helped us to run the simulation ensemble on the PC-based cluster of the laboratory. Thanks are also due to E. Mansell (CIMMS, University of Oklahoma, Oklahoma) for providing us with the multicell case sounding.

REFERENCES

Altaratz, O., T. Reisin, and Z. Levin, 2005: Simulation of the electrification of winter thunderclouds using the three-dimensional regional atmospheric modeling system (RAMS) model: Single cloud simulations. *J. Geophys. Res.,* **110,** D20205, doi:10.1029/2004JD005616.

Barthe, C., and J.-P. Pinty, 2007a: Simulation of a supercellular storm using a three-dimensional mesoscale model with an explicit lightning flash scheme. *J. Geophys. Res.,* **112,** D06210, doi:10.1029/2006JD007484.

——, and ——, 2007b: Simulation of electrified storms with comparison of the charge structure and lightning efficiency. *J. Geophys. Res.,* **112,** D19204, doi:10.1029/2006JD008241.

——, G. Molinié, and J.-P. Pinty, 2005: Description and first results of an explicit electrical scheme in a 3D cloud resolving model. *Atmos. Res.,* **76,** 95–113.

——, J.-P. Pinty, and C. Mari, 2007: Lightning-produced NO_x in an explicit electrical scheme: A STERAO case study. *J. Geophys. Res.,* **112,** D04302, doi:10.1029/2006JD007402.

DeCaria, A. J., K. E. Pickering, G. L. Stenchikov, and L. E. Ott, 2005: Lightning-generated NO_x and its impact on tropospheric ozone production: A three-dimensional modeling study of a Stratosphere-Troposphere Experiment: Radiation, Aerosols, and Ozone (STERAO-A) thunderstorm. *J. Geophys. Res.,* **110,** D14303, doi:10.1029/2004JD005556.

Defer, E., P. Laroche, J. E. Dye, and W. Skamarock, 2003: Use of total lightning lengths to estimate NO_x production in a Colorado thunderstorm. *Extended Abstract, 12th Int. Conf. on Atmospheric Electricity,* Versailles, France, International Committee on Atmospheric Electricity, 583–586.

Fehr, T., H. Holler, and C. Théry, 2004: Model study on production and transport of lightning-produced NO_x in a EULINOX supercell storm. *J. Geophys. Res.,* **109,** D09102, doi:10.1029/2003JD003935.

Helsdon, J. H., Jr., W. A. Wojcik, and R. D. Farley, 2001: An examination of thunderstorm-charging mechanisms using a two-dimensional storm electrification model. *J. Geophys. Res.,* **106** (D1), 1165–1192.

Houtekamer, P. L., and J. Derome, 1995: Methods for ensemble prediction. *Mon. Wea. Rev.,* **123,** 2181–2196.

Huntrieser, H., H. Schlager, C. Feigl, and H. Holler, 1998: Transport and production of NO_x in electrified thunderstroms: Surveys of previous studies and new observations at midlatitudes. *J. Geophys. Res.,* **103,** 28 247–28 264.

Klemp, J. B., and R. B. Wilhelmson, 1978: The simulation of three-dimensional convective storm dynamics. *J. Atmos. Sci.,* **35,** 1070–1096.

Krehbiel, P., R. J. Thomas, W. Rison, T. Hamlin, J. Harlin, and M. Davis, 2000: A GPS-based mapping system reveals lightning inside storms. *Eos, Trans. Amer. Geophys. Union,* **81,** 21–25.

Lee, D. S., and Coauthors, 1997: Estimations of global NO_x emissions and their uncertainties. *Atmos. Environ.,* **31,** 1735–1749.

MacGorman, D. R., J. M. Straka, and C. L. Ziegler, 2001: A lightning parameterization for numerical cloud models. *J. Appl. Meteor.,* **40,** 459–478.

Mansell, E. R., D. MacGorman, C. L. Ziegler, and J. M. Straka, 2002: Simulated three-dimensional branched lightning in a numerical thunderstorm model. *J. Geophys. Res.,* **107,** 4075, doi:10.1029/2000JD000244.

——, ——, ——, and ——, 2005: Charge structure and lightning sensitivity in a simulated multicell thunderstorm. *J. Geophys. Res.,* **110,** D12101, doi:10.1029/2004JD005287.

Marshall, T. C., M. P. MacCarthy, and W. D. Rust, 1995: Electric field magnitudes and lightning initiation in thunderstorms. *J. Geophys. Res.,* **100,** 7097–7103.

Niemeyer, L., L. Pietronero, and H. J. Wiesmann, 1984: Fractal dimension of dielectric breakdown. *Phys. Rev. Lett.,* **52,** 1033–1036.

Ott, L. E., K. E. Pickering, G. L. Stenchikov, H. Huntrieser, and U. Schuman, 2007: Effects of lightning NO_x production during the 21 July European Lightning Nitrogen Oxides Project storm studied with a three-dimensional cloud-scale chemical transport model. *J. Geophys. Res.,* **112,** D05307, doi:10.1029/2006JD007365.

Skamarock, W. C., J. E. Dye, E. Defer, M. C. Barth, J. L. Stith, B. A. Ridley, and K. Baumann, 2003: Observational- and modeling-based budget of lightning-produced NO_x in a continental thunderstorm. *J. Geophys. Res.,* **108,** 4305, doi:10.1029/2002JD002163.

Takahashi, T., 1978: Riming electrification as a charge generation mechanism in thunderstorms. *J. Atmos. Sci.,* **35,** 1536–1548.

Wang, Y. A., W. DeSilva, G. C. Goldenbaum, and R. R. Dickerson, 1998: Nitric oxide production by simulated lightning: Dependance on current, energy and pressure. *J. Geophys. Res.,* **103,** 19 149–19 159.

Weisman, M. L., and J. B. Klemp, 1984: The structure and classification of numerically simulated convective storms in directionally varying wind shear. *Mon. Wea. Rev.,* **112,** 2479–2498.